Journal of Structural Chemistry. Vol. 58, No. 5, pp. 953-963, 2017.

THE USE OF 2D DIFFRACTOMETRY DATA FOR ORIENTED SAMPLES IN THE CHOICE OF A UNIT CELL

A. S. Sukhikh[1,2], T. V. Basova[1,2], and S. A. Gromilov[1,2]

UDC 548.734

An approach for the substantiated choice of the indexing procedure of a diffraction pattern is described. The technique is based on a combined use of powder X-ray diffraction data in Bragg–Brentano schemes and 2D GIXD of mainly oriented polycrystalline samples.

DOI: 10.1134/S0022476617050146

Keywords: X-ray diffractometry of polycrystals, oriented samples, thin films, indexing, palladium phthalocyanines.

INTRODUCTION

The problem of correct indexing of experimental diffraction pattern and the determination of symmetry and unit cell parameters (UCPs) is one of the main problems of the X-ray crystallographic analysis of polycrystals. This problem can be due to: impossibility to obtain quality single crystals for the classical X-ray crystallographic analysis; non-single phase sample; large and close (including multiple) UCPs; great (several times) difference in linear parameters *a*, *b*, *c*; small deviations of angular parameters α, β, γ from 60°, 90°, or 120°. Despite that modern diffractometers for the analysis of polycrystals and the respective processing programs enable the determination of the position of reflection maxima with an accuracy up to 0.01° 2θ, the indexing often yields several equivalent variants. This situation requires the attraction of additional data, such as microcrystal faceting (if any), density (if a smaple is single-phase), electron microdiffraction (if the phase is not destructed by an electron beam), synchrotron radiation diffraction (if used). The latter approach is most promising because it allows the studies of crystals with a size up to 0.1 μm, however, we are far from the routine use of synchrotron radiation and perfect single crystals (even so small) not always can be obtained.

When performing X-ray crystallographic analysis of transition metal phthalocyanines (TMPs) a researcher faces almost all mentioned problems: large single crystals do not grow (especially for metastable crystalline phases), great difference in UCPs, low crystal symmetry, occurrence of several modifications [1-3]. Therefore, at present only single cases of the complete structure solution have been known. This forces the researchers to study polycrystals, however, additional problems arise here, such as significant texturization, overlap of reflections, and the diffraction pattern breaks up already at 25° 2θ. The latter makes practically impossible to search for reflections characterizing the shortest linear parameter (usually it is in the range 3.5-4.5 Å). In this situation the application of automatic search methods for UCPs from a small number of

[1]Nikolaev Institute of Inorganic Chemistry, Siberian Branch, Russian Academy of Sciences, Novosibirsk, Russia; a_sukhikh@niic.nsc.ru. [2]Novosibirsk National Research State University, Russia. Translated from *Zhurnal Strukturnoi Khimii*, Vol. 58, No. 5, pp. 992-1002, June-July, 2017. Original article submitted December 20, 2016.

reflections can result in dubious indexing variants, e.g. in [4, 5] UCPs of a triclinic cell were determined based on only 7-8 reflections.

Another aspect in the study of TMPs is associated with the examination of their properties in devices where they are analyzed as thin layers. Since these compounds are volatile, then for the preparation of these layers chemical vapor deposition is applied. Usually, oriented polycrystalline samples form as a result [6-9]. Their state can be characterized as intermediate between single and polycrystalline. A characteristic feature of the diffraction pattern obtained from these samples in the Bragga–Brentano geometry is the presence of only one diffraction reflection corresponding to the distinguished crystallographic direction. Vacuum deposited TMP layers almost always represent a certain crystal modification, unlike the precursor that is usually multiphase. Thus, the X-ray diffraction information obtained just from the TMP layer can become especially important for the solution of a number of crystal structural problems.

In [10] it was shown that for the X-ray diffraction identification of a phase in the form of an oriented layer the 2D grazing incidence X-ray diffraction (2D GIXD) geometry with a two-coordinate detector could be used [11-14]. This technique differs from the classical grazing incidence scheme [15, 16] assuming that the one-dimensional diffraction pattern is fixed. The use of a two-coordinate detector makes it possible to fix reflections from the focusing circle plane. Thus, in the study of an only 37 nm thick ideally oriented CoPc layer the authors of [10] managed to obtain the positions of these several additional reflections and unambiguously identify the phase as the α-modification of CoPc [10]. The application of this procedure in determining the degree of crystallinity of oriented films was described in [17]. In [18] by the comparison of 2D GIXD diffraction patterns it was shown that tetrasubstituted cobalt phthalocyanine ($CoPcF_4$) is isostructural to α-CoPc, and the diffraction pattern of $CoPcF_4$ was indexed based on it.

In this publication we propose a further development of the procedure in terms of a combined use of sufficiently accurate data obtained in the Bragg–Brentano scheme and less accurate 2D GIXD data, but containing additional crystal structural information. This information is the angles between the crystallographic planes. The determination of a series of these angles provides the verification of the indexing, i.e. to reasonably choose the correct variant among several equivalent ones. Another variant is the use of only 2D GIXD data for the oriented sample, it being simply a sample with appreciable preferred orientation. When the number of reflections in the 2D diffraction pattern is sufficient, it is possible to expect to obtain five UCPs (two linear and three angular). In this work the solution of the posed problems is demonstrated on the example of tetrafluorinated palladium phthalocyanine ($PdPcF_4$) and hexadecafluorinated palladium phthalocyanine ($PdPcF_{16}$) (Fig. 1). For both phases the crystal structural information is absent. For PdPc (all periphery hydrogen atoms) the existence of two crystalline phases has been known: stable high-temperature β-PdPc [19] and metastable α-PdPc [20].

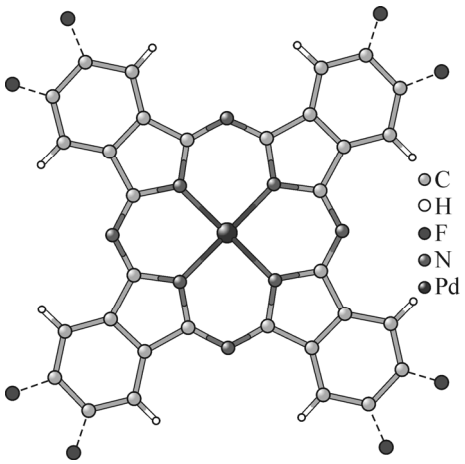

Fig. 1. $PdPcF_4$ molecule. A dashed line shows the fluorine atoms disoriented over two positions. In the $PdPcF_{16}$ molecule all periphery atoms are the fluorine atoms.

EXPERIMENTAL

$PdPcF_4$ was obtained by heating a mixture of 4-fluorophthalo-1,2-dinitrile (99% Sigma-Aldrich) and anhydrous palladium(II) chloride (99.9% Sigma-Aldrich) in an ampoule to 220 °C for 6 h. The product obtained was then twice purified in a gradient furnace by vacuum zone sublimation. The synthesis of the initial polycrystalline product $PdPcF_{16}$ was described in [20].

$PdPcF_4$ and $PdPcF_{16}$ layers were thermally deposited under the same conditions using a Knudsen chamber (residual pressure ~$1.5 \cdot 10^{-5}$ mBar, 450 °C). Glass slabs with a thickness of 0.1 mm were used as substrates. The obtained layers were no more than 100 nm thick.

A measurement in the GIXD geometry assumes the exposure of a sample with a narrow parallel X-ray beam at a grazing angle (Fig. 2). In our case, this geometry was implemented based on a single crystal Bruker DUO diffractometer equipped with a 2D CCD detector and an Incoatec IμCu microfocus tube with a copper anode (0.25 mm and 0.6 mm exchangeable collimators) [17]. The sample under study was fixed by a special adapter and centered by the standard video camera. The sample turn relative to the primary beam was set by changing the φ angle, with other setting angles of the goniometer (ω, χ) being 0. Thus, the measurement geometry was similar to that on a horizontal type goniometer with the vertical placement of a sample. For the convenience of further processing the diffraction patterns were fixed at a zero turn angle of the detector ($2\theta_D = 0$). A transition to the standard form of the diffraction pattern (integration) was made in the XRD2DScan 4.1.1 program [21].

To measure in the 2D GIXD geometry it is needed to choose the optimal conditions: φ incident angle of the primary beam on the sample, primary beam width (determined by the collimator diameter), and the distance from the sample to the detector *L*. The correct choice provides the required characteristics of the diffraction pattern (resolution, intensity, diffraction angle range) in reasonable time.

Choice of the optimal distance to the detector. The distance between the detector and the sample (*L*) affects not only the intensity of the diffraction pattern but also the width of the observed diffraction reflections. The choice of the optimal *L* value is always a search for the compromise between the intensity of the diffraction pattern and its resolution. In our case, the goniometer enables the variation of *L* in the range 35÷180 mm with an accuracy of 0.01 mm.

For the substantiated choice of *L* two series of measurements of the reference were performed using collimators with different diameters (∅). The distance *L* was increased from 40 mm to 160 mm with a step of 5 mm. A small

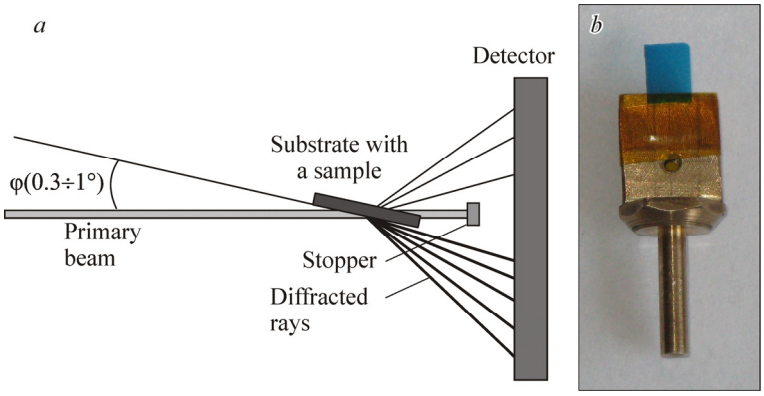

Fig. 2. Measurement scheme in the 2D GIXD geometry: primary X-ray beam is incident at an acute φ angle on the sample surface; diffracted rays are fixed by a planar detector; part of rays passes through the substrate material and is noticeably weakened (*a*); sample in the form of a fragment of a thin glass slab fixed on the adapter by polyimide adhesive tape (*b*).

(~0.3×0.3×0.05 mm) chip of α-Al_2O_3 corundum ceramics was used as a sample (NIST SRM-1976b reference). The detector was turned at –25.57° 2θ so that the (012) line of corundum was fixed by the central part of the detector, and errors due to its tilt were minimum. The dependences of the full width at half maximum (FWHM) and the intensity (the XRD2DScan program averages the intensity over the whole diffraction ring) of the observed line on L are shown in Fig. 3.

In the entire L range the use of a collimator with ∅ = 0.25 mm, as compared to 0.6 mm, makes it possible to obtain smaller FWHM by approximately 0.1° (Fig. 3*a*). In both cases, a main decrease in FWHM (approximately 1.7 times) occurs in the range from 40 mm to 80 mm. The intensity decreases approximately equally (Fig. 3*b*). At a further increase in the distance from 80 mm to 160 mm FWHM asymptotically reaches 0.3° for ∅ = 0.6 mm and 0.2° for ∅ = 0.25 mm. Concurrently, the intensity decreases approximately three times. Thus, after 80 mm the FWHM gain becomes less and less significant. The graphs permit the choice of two optimal combinations ∅/L: 0.6/80 to obtain the highest intensity and 0.25/120 to obtain the best resolution. Being guided by the former aspect, we used the 0.6 mm collimator and L = 80 mm in the study of thin TMP layers.

Choice of the optimal primary beam incident angle. In the study of a thin layer in the 2D GIXD geometry the main parameter determining the measurement of the diffraction pattern is the primary beam incident angle. The intensity of the observed diffraction pattern and the background intensity from the substrate material depend on this parameter. At large angles a part of the diffraction pattern can be shadowed by a substrate. At too acute angles the diffraction pattern intensity abruptly decreases because only part of the primary beam is incident on the sample while the most part is scattered by the substrate, which increases the background. Thus, the problem arises of determining the optimal beam incident angle that would provide the extremely qualitative data with a reasonable duration of the experiment. The main problem is the absence of the technique enabling the accurate measurement of the angle between the beam and the substrate plane.

The goniometer allows the rotation of the fixed sample about the φ axis at an arbitrary angle with good accuracy and reproducibility (+/–0.001°). However, the sample position at which its plane coincides with the primary beam can be monitored only visually by the standard video camera whose shallow depth of field does not make it possible to precisely fix the positions of substrate ends at 180° turns about the φ axis. To determine the real incident angle we used the optical reflection of the primary beam from the substrate surface. The essence of this phenomenon consists in that when the X-ray beam is incident on a sufficiently smooth surface at small angles, part of the beam reflects from this surface as from the mirror. This is manifested as an additional reflection in the diffraction pattern, the reflection angle equals the double primary beam incident angle. Fig. 4 depicts the fragments of diffraction patterns of $PdPcF_4$ at different φ angles in the range 0÷3 with a step of 0.2°. It is well seen that the position of the diffraction reflection of $PdPcF_4$ remains unchanged whereas the spot due to the primary beam reflection gradually loses the intensity and shifts to larger angles.

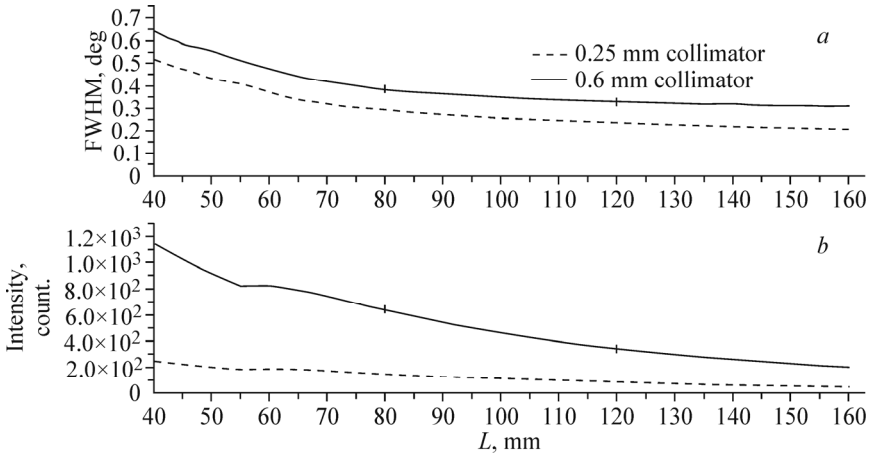

Fig. 3. Dependence of the half-width (*a*) and intensity (*b*) of the corundum (012) line on the distance to the detector.

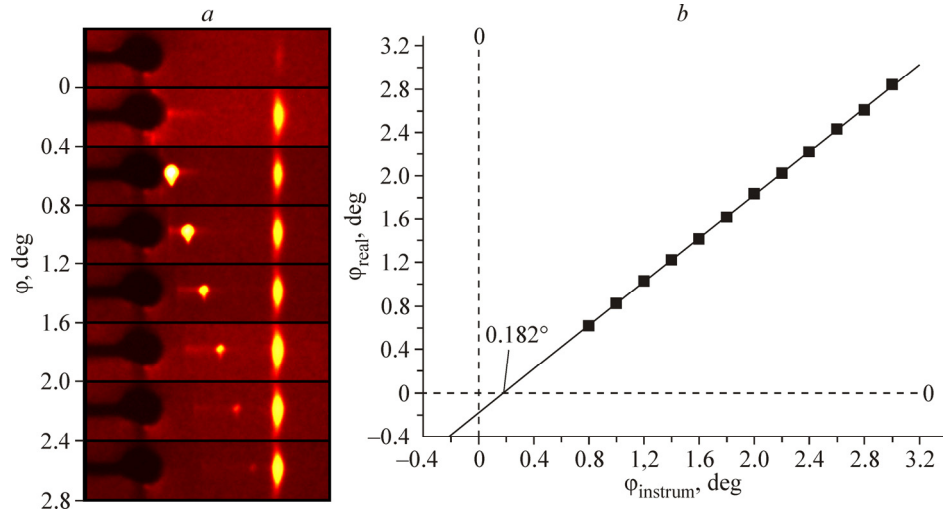

Fig. 4. To the determination of the primary beam incident angle: fragments of diffraction patterns of $PdPcF_4$ at different φ rotation angles of the sample (in the two upper figures a spot due to the primary beam reflection is cut off by a stopper (*a*); dependence of the primary beam reflection angle on the sample rotation angle (*b*).

Fig. 4*b* shows the dependence of the angular position of the primary beam reflection on the sample rotation angle. This dependence can be described by the linear equation $\varphi_{real} = 1.003(3)\times\varphi_{instrum} - 0.182°(8)$. As a result it is found that the zero position of the sample should be considered φ = 0.182°.

After the determination of the zero position of the sample it is possible to construct the dependence of the intensity of diffraction spots and the background level on the sample rotation angle. Fig. 5 depicts these dependences for the reflections from $PdPcF_4$ crystallites oriented parallel to the substrate plane. The highest background point in the diffraction pattern (after smoothing the frame to eliminate local surges and hot pixels) as a criterion of the background intensity.

From the obtained graphs it is seen that the intensity drastically increases in the range 0.2-0.3° φ. In the linear region from 0.3° to 3.7° there is a four times increase. Here the background level remains practically the same and only slightly decreases with increasing φ. An increase in φ by more than 4° causes a decrease in the intensity and an increase in the background level, furthermore, a shadow from the substrate (it is well seen in Fig. 4) covers a large area of the diffraction pattern. Thus, in this case, the optimal φ range can be considered to be the one from 0.3° to ~3.7°.

Sample centering. Since the goniometric head of the BRUKER DUO diffractometer is intended to mount and center small (up to 1 mm) single crystals, significant problems arise in mounting our samples (substrates with deposited layers) whose sizes reach 5 mm (Fig. 6).

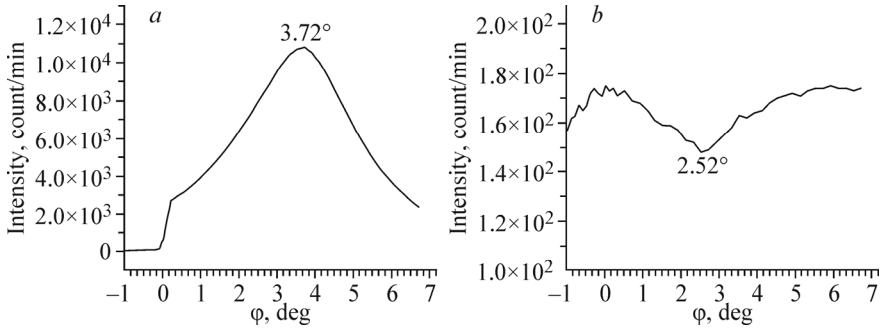

Fig. 5. Dependence of the diffraction spot intensity of $PdPcF_4$ with d = 13.56 Å on the φ angle (*a*); dependence of the background level on the φ angle (*b*).

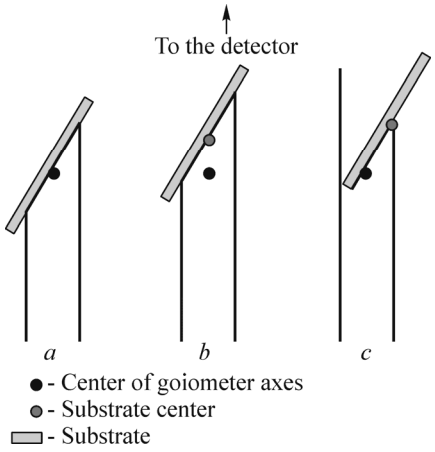

Fig. 6. Possible variants of the sample positioning relative to the primary beam: correct positioning (*a*); sample surface does not pass through the goniometer axis (*b*); sample center is shifted from the goniometer axis (*c*).

If the sample is mounted correctly, then the centers of the primary beam and the sample and the φ axis coincide (Fig. 6*a*). In this case, the real coordinates of the center of the obtained diffraction pattern and the distance to the detector coincide with the instrumental values. In the second variant (Fig. 6*b*), the centers of the primary beam and the sample lie on one straight line, however, the substrate is closer (another variant – farther) to the detector. This centering error results in the incorrect distance L between the detector and the sample and the respective systematic error. The attempt to process these data without introducing the distance correction leads to an increase/decrease in angular positions of all observed diffraction spots. In the latter case (Fig. 6*c*), the primary beam mainly lights up the nearest (another variant – farthest) part of the sample. In this situation, the center of the observed diffraction pattern is shifted relative to the instrumental zero. As practice shows, in our experiments this shift does not exceed 5 pixels (i.e. 0.3 mm). However, even such a minor deviation in the integration of the diffraction pattern causes a noticeable distortion of the peak shapes and their shifts, especially in the 2θ angle range less than 10°. Since in our case, the sample is placed vertically, the diffraction pattern is mainly shifted along the X coordinate whereas the Y coordinate remains almost unchanged. The axis directions are shown in Fig. 7.

Due to the geometric features of the 2D GIXD scheme the pattern has the C_{2v} symmetry. This can be used to correct the sample centering. In the 2D GIXD pattern (Fig. 7*a*) four symmetrically related reflections correspond to each *hk*0 set and two to *h*00 taken parallel to the substrate plane.

The center of the diffraction pattern can be roughly defined as an intersection point of straight lines drawn through the centers of *hk*0 symmetric diffraction spots. However, the low intensity of spots in the left (shadowed by the substrate) half of the frame does not always provide the sufficiently accurate determination of their centers. Furthermore, in some cases, the intensity of reflections is so low that they all, except *h*00 (marked by a white oval in Fig. 7*a*), are simply absent in the left part of the frame. In this case, to determine the center it is possible to compare in pairs the 2θ angles for all symmetrically related reflections only in the right part. If the center is found correctly, then the 2θ values for each pair must coincide. Otherwise the center coordinates must be shifted to a reflection with larger 2θ. This approach enables the manual iterative refinement of the coordinates of the detector center.

For example, let us describe a search for the center of the diffraction pattern of $PdPcF_{16}$ in Fig. 7*a*. Instrumental (i.e., found as a result of the goniometer adjusting) coordinates of the detector zero were used as the starting values: $X = 514.44$, $Y = 508.78$. In processing the regions marked by blue ovals the following 2θ values were obtained for four symmetrically related reflections: 6.14° (*a*), 6.42° (*b*), 6.47° (*c*), and 6.19°(*d*). Apparently, the real center of the diffraction pattern is

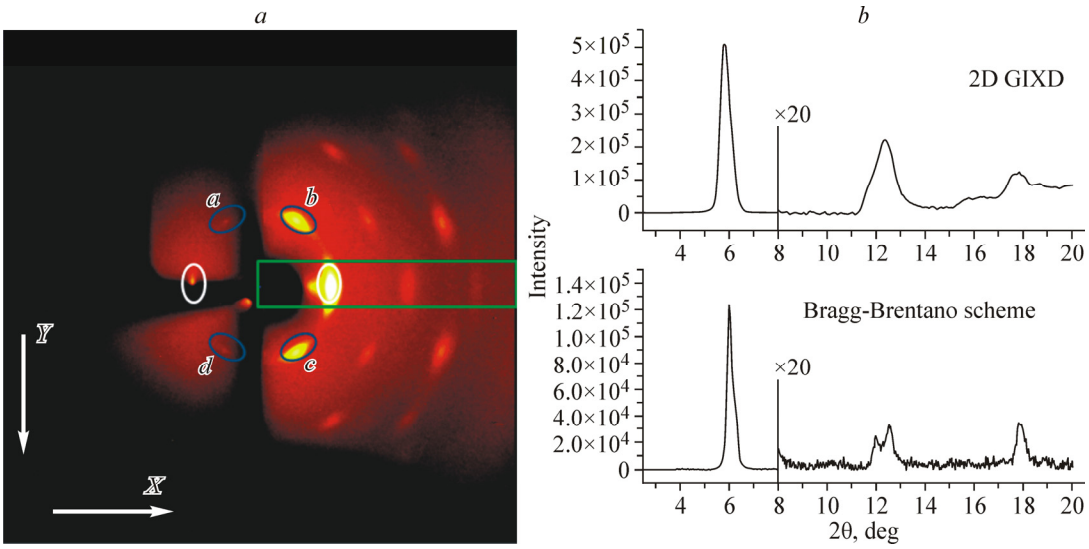

Fig. 7. Diffraction patterns of $PdPcF_{16}$: 2D GIXD pattern (blue ovals mark four symmetrically related reflections) (*a*); comparison of the diffraction patterns obtained by different schemes (2θ region from 8° to 20° is shown with a 20-fold magnification) (*b*). A gray rectangle depicts the integration region.

somewhere lower on the *Y* axis and much to the right of the *X* axis. After several iterations the following coordinates of zero were obtained: $X = 518.9$, $Y = 508.8$. The 2θ values for the diffraction spots were: 6.294° (*a*), 6.298° (*b*), 6.301° (*c*), and 6.294° (*d*). Now the 2θ values differ only by thousandths of degrees. The center coordinates changed by 4.5 pixels on *X* and only by 0.02 pixels on *Y*. A small shift along the *Y* axis is characteristic of 2D GIXD patterns and is due to the vertical placement of the sample.

After the determination of the accurate coordinates of the center of the diffraction pattern a correction for the distance between the sample and the detector (*L*) can be calculated. To this end, a fragment of frame marked by a green rectangle in Fig. 7*a* was integrated. The range approximately corresponds to the measurement range of the diffraction pattern in the Bragg–Brentano scheme. A comparison of the diffraction patterns (Fig. 7*b*) makes it possible to determine the shift of the diffraction reflection in the 2D GIXD pattern. If the distance between the sample and the detector is chosen correctly, then the positions of diffraction peaks must coincide in both diffraction patterns. If the peak positions differ by some Δ2θ value, then the correction can be calculated as

$$\Delta L = L\left(\frac{\mathrm{ctg}(2\theta + \Delta 2\theta)}{\mathrm{ctg}(2\theta)} - 1\right).$$

Data processing. The obtained diffraction patterns (with regard to the above corrections) can be processed, e.g., in the XRD2DScan 4.1.1 program. Fig. 8*a* shows the 2D GIXD pattern of $PdPcF_4$. At the first stage, the integration over 2θ in a narrow sector (marked with white) containing the selected diffraction spot was carried out and the position of the maximum was found based on the obtained diffraction pattern. Now knowing the 2θ value, for the selected spot the integration over φ was carried out in the range +/–0.3° 2θ (the range was chosen as equal to the half-width of the diffraction peak) from its maximum (Fig. 8*b*). For the symmetrically related diffraction spots the average values were used (Fig. 8*c*), which are the angles between the selected crystallographic plane and the preferred orientation plane.

All mentioned procedures were used in the processing of diffraction patterns of $PdPcF_4$ and $PdPcF_{16}$ thin layers.

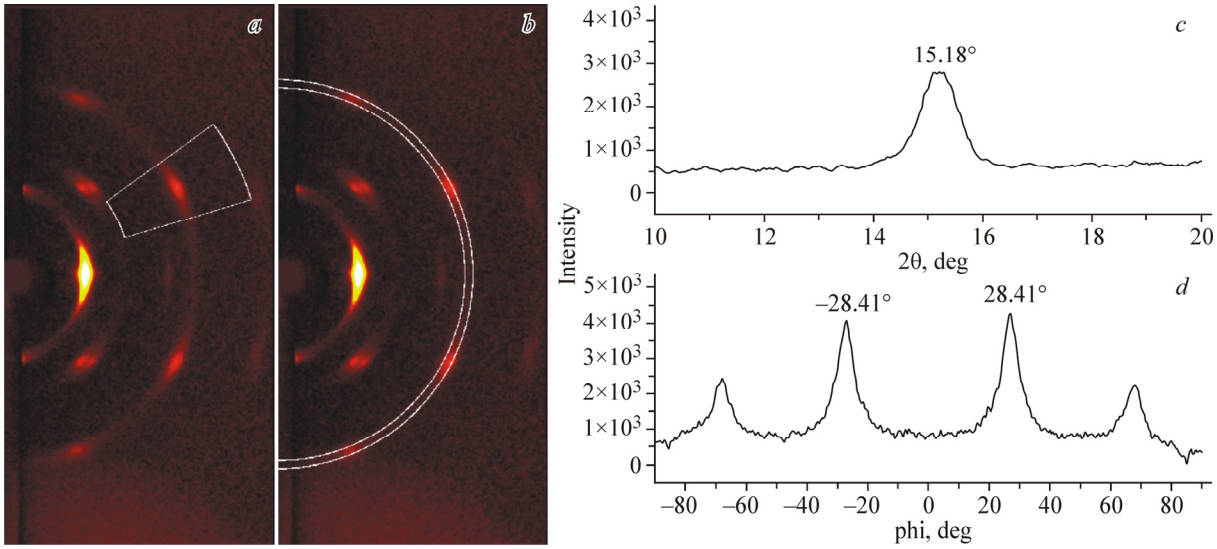

Fig. 8. Processing of 2D GIXD data for $PdPcF_4$: sector selected for the integration over 2θ (*a*); sector for the integration over φ (*b*); determination of the position with respect to 2θ (*c*); determination of the position with respect to φ (*d*) (the depicted values are the angles between the chosen crystallographic plane and the preferred orientation plane).

RESULTS AND DISCUSSION

Determination of UCPs of $PdPcF_4$. Diffraction patterns (Shimadzu-7000, CuK_α radiation, Ni filter, Bragg–Brentano scheme) of a $PdPcF_4$ polycrystalline sample and its layer are presented in Fig. 9. In both cases, the total acquisition time was ~15 h. A polycrystalline corundum sample (α-Al_2O_3) was used as the internal reference. The positions of main lines (2θ = 6.51°) coincide in both diffraction patterns; five orders of this reflection can be traced in the diffraction patterns of thin layers. As a result of processing the diffraction pattern of $PdPcF_4$ by the Origin9 program it was possible to find the positions of maxima of 44 diffraction peaks in the angle range 6÷40°. The attempts of indexing from the first 20 peaks by means of the

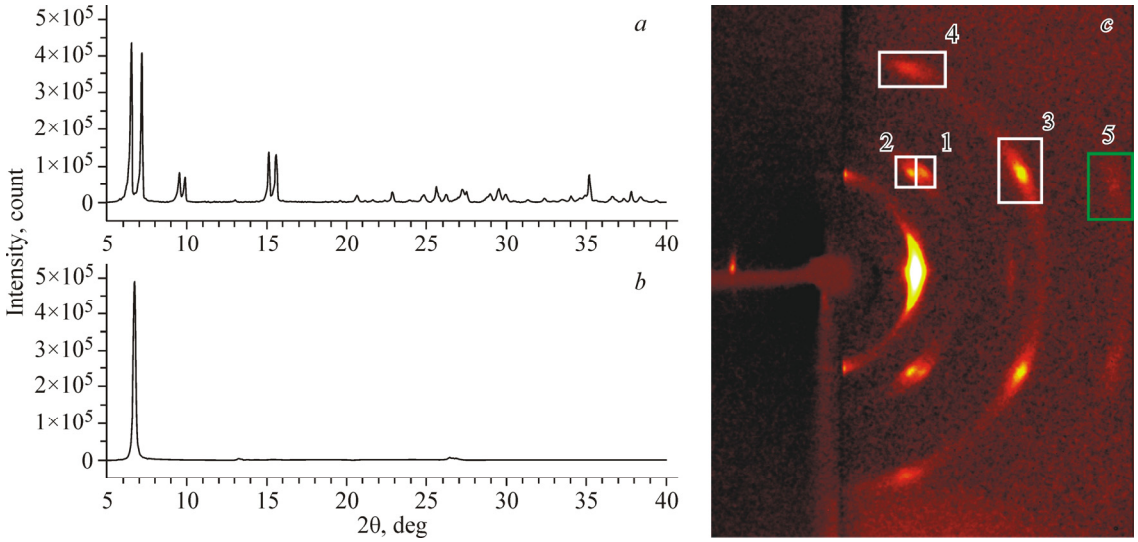

Fig. 9. Diffraction patterns of $PdPcF_4$ (Shimadzu-7000, CuK_α radiation, Ni filter, Bragg–Brentano scheme): polycrystalline sample (*a*); layer on a glass substrate (*b*); 2D GIXD diffraction pattern of the $PdPcF_4$ layer (*c*). White rectangles single out four spots for which the σ angles were measured. A gray rectangle marks the spot that is distinguishable but too smeared for the accurate measurement.

Dicvol06 program gave a large number (>30) of UCP variants with acceptable quality criteria. In this situation it is impossible to unambiguously make a choice in favor of that or another variant. Table 1 summarizes three variants of indexing; for all of them the quality criteria (F_{24}) were calculated based on the first 24 reflections. Crystal chemical arguments on the possible volume of the $PdPcF_4$ molecule (a rule of 18 Å^3 cell volume per atom, except hydrogen) yield a value of 810 Å^3, which better agrees with the unit cell volume of variant 3. However, after the processing of the 2D GIXD diffraction pattern and the determination of σ angles between the basic plane and the crystallographic planes (their numbers are shown in Fig. 9, the reflection under number 5 is observed but has too low intensity to accurately determine the position). Variant 3 was rejected. The diffraction pattern of a $PdPcF_4$ layer on a glass substrate, which was obtained in the 2D GIXD geometry, is presented in Fig. 9*c*. It was obtained under the following conditions: primary beam incident angle φ = 1°, *L* = 80 mm, collimator diameter 0.6 mm, acquisition time 1 h.

As seen from Table 1, in variants 1 and 2 the σ angles are well consistent with the experimental data (a deviation does not exceed 0.15°). For both variants the calculated interplanar angles are almost identical. This indicates that even with increasing determination accuracy of σ angles four values would be insufficient for the unambiguous choice. In this situation it is possible to use an analogy with α-CoPc and $CoPcF_4$ [5]. The triclinic unit cell volume of $CoPcF_4$ (605 Å^3) is larger than that of α-CoPc (578 Å^3) by 27 Å^3. Assuming that the α-PdPc and $PdPcF_4$ unit cells are related, it is possible to expect the $PdPcF_4$ unit cell to be triclinic and have a volume of ~619 Å^3 (the α-PdPc unit cell volume is 592 + 27 Å^3). Thus, variant 1 seems more preferable.

Determination of $PdPcF_{16}$ UCPs. Diffraction patterns of $PdPcF_{16}$ samples obtained in the Bragg–Brentano scheme are shown in Fig. 10*a*, *b*. A pronounced complex multiplet in the 2θ range 5-7° in the diffraction pattern of the initial polycrystalline sample indicates a complex phase composition: the product contains at least two crystalline phases with comparable UCPs. In this situation, the indexing seems to be impossible. At the same time, the diffraction pattern of the $PdPcF_{16}$ layer has the form characteristic of a single-phase oriented sample. To estimate UCPs a 2D diffraction pattern (Fig. 10*c*) was used, which was measured at a primary beam incident angle of 0.3° and *L* = 80 mm. In this case, a collimator with ∅ 0.25 mm was applied, which improved the diffraction pattern resolution but at the same time, increased the measurement time to 15 h.

By assigning (100) and (001) indices to the reflections with the largest *d* values in the 2D GIXD pattern, the other reflections were indexed. As seen in the inset, the (–100) and (101) reflections merge, therefore they were not used further. Then the interplanar distances were corrected based on the diffraction pattern measured in the Bragg–Brentano scheme (values are given in Table 2 in parentheses). Using nine independent experimental parameters marked with bold (five interplanar distances and four σ angles) five out of six UCPs were estimated: $a \approx 15.4$ Å, $c \approx 16.4$ Å, $\alpha \approx 87°$, $\beta \approx 63°$, $\gamma \approx 88°$. In the last two columns of Table 2 the calculated σ and 2θ angles are given for verification.

TABLE 1. Comparison of Indexing Variants for the Diffraction Pattern of $PdPcF_4$

Characteristic		Variant 1	Variant 2	Variant 3
Crystal symmetry		Triclinic	Monoclinic	Triclinic
a, *b*, *c*, Å		12.39(4), 3.74(2), 13.68(5)	12.329(3), 3.610(3), 13.605(4)	13.61, 5.42, 13.70
α, β, γ, deg		84.14(1), 87.325(6), 84.603(6)	90, 92.147(5), 90	64.31, 92.42, 91.13
V, Å^3		630	605	910
F_{24} (n_{poss})		54.8 (34)	74.1 (29)	95.6 (56)
$\lvert\Delta 2\theta\rvert_{24}$, deg		0,013	0,011	0,0044
σ_1, deg	46.49_{exp}	46.63 (–101)	46.64 (101)	41.25 (101)
σ_2, deg	48.87_{exp}	48.99 (101)	49.00 (–101)	43.18 (–101)
σ_3, deg	28.41_{exp}	28.37 (–102)	28.38 (102)	24.76 (–102)
σ_4, deg	67.52_{exp}	67.41 (201)	67.42 (–201)	62.79 (–201)

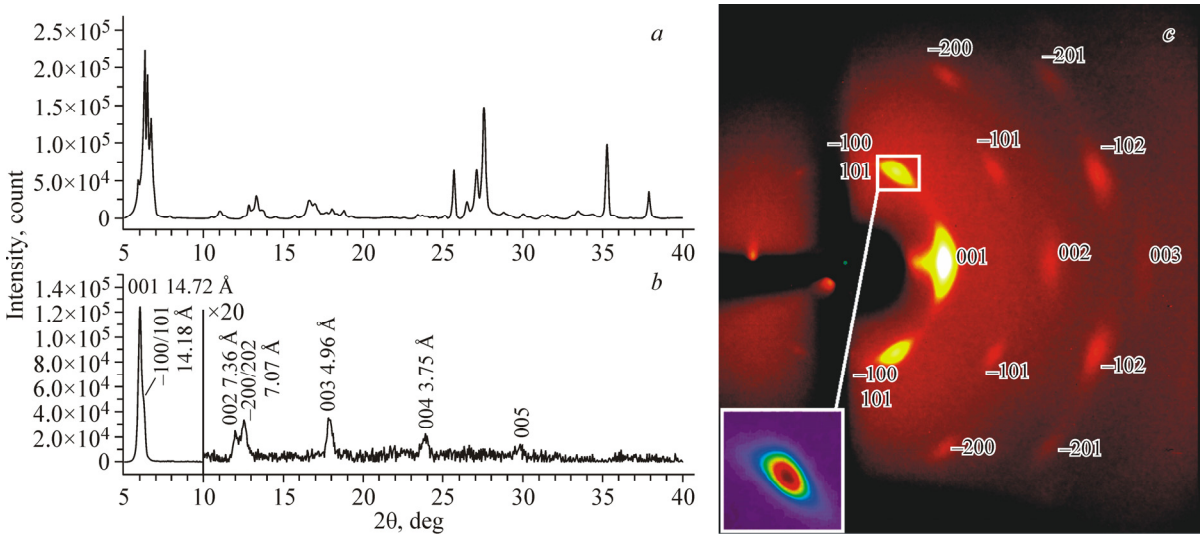

Fig. 10. Diffraction patterns of $PdPcF_{16}$ samples: initial polycrystalline sample (*a*); layer on a glass substrate (the 2θ region from 10° to 40° is depicted with a 20-fold magnification) (*b*); 2D GIXD pattern (*c*). A distorted shape of the diffraction spot in the inset is caused by the superposition of spots from the (101) and (–100) planes.

TABLE 2. Powder X-ray Diffraction Characteristics of $PdPcF_{16}$ According to the 2D GIXD Data

No.	$2\theta_{exp}$, deg	d_{exp}, Å	*hkl*	σ_{exp}, deg	σ_{calc}, deg	$2\theta_{calc}$, deg
1	5,96	14,83 (**14,72**)*	001	0	0	6,13
2	11,90	7,44 (**7,37**)*	002	0	0	12,13
3	17,90	4,96 (**4,96**)*	003	0	0	18,47
4	6,29	14,05 (**14,18**)*	–100 / 101	62,6	63,06 / 61,37	6,44 / 6,54
5	12,92	***6,85***	–200	***62,3***	63,06	12,90
6	10,72	***8,25***	–101	***32,2***	32,62	10,66
7	16,09	***5,51***	–102	***19,6***	20,91	16,13
8	16,57	***5,35***	–201	***42,2***	44,01	16,58

* In parentheses the values obtained in the Bragg–Brentano scheme are given.

CONCLUSIONS

A combination of the ultra-bright microfocus tube and the 2D CCD detector enabled an efficient implementation of the 2D GIXD geometry in the standard single crystal diffractometer and the investigation of the diffraction of ~100 nm thick oriented layers. A complex of measures was proposed to compensate distortions of the obtained experimental data due to the incorrect positioning of the sample and the detector. By the example of studying $PdPcF_4$ thin layers it was shown that additional data on the angles between the crystallographic planes made it possible to exclude knowingly wrong variants of UCPs. The combined use of the powder X-ray diffraction data on the oriented $PdPcF_{16}$ layer, which were obtained in the Bragg–Brentano geometry, and 2D GIXD provided the reliable information about five parameters of the triclinic unit cell. The described approach can be used in the study of phase transitions occurring in thin layers of TMPs with changing external conditions.

The authors are grateful to D. D. Klyamer and Dr. R. G. Parkhomenko for granting the samples.

The work was supported by the Russian Scientific Foundation (project No. 15-13-10014).

REFERENCES

1. G. A. Williams, B. N. Figgis, R. Mason, S. A. Mason, and P. E. Fielding, *J. Chem. Soc. Dalton Trans.*, **9**, 1688 (1980).
2. P. Ballirano, R. Caminiti, C. Ercolani, A. Maras, and M. A. Orru, *J. Am. Chem. Soc.*, **120**, 12798 (1998).
3. H. Jiang, J. Ye, P. Hu, F. Wei, K. Du, N. Wang, T. Ba, S. Feng, and C. Kloc, *Sci. Rep.*, **4**, 7573 (2014).
4. I. Dhanya and C. S. Menon, *Vacuum*, **86**, 1289-1295 (2012).
5. N. S. Lebedeva, E. V. Parfenyuk, and E. A. Malkova, *Spectrochim. Acta A*, **68**, No. 3, 491-494 (2007).
6. M. M. El-Nahhas, Z. El-Gohary, and H. S. Soliman, *Opt. Laser Technol.*, **35**, 523 (2003).
7. T. Sizun, M. Bouvet, Y. Chen, J. M. Suisse, G. Barochi, and J. Rossignol, *Sens. Actuators, B*, **159**, 163-170 (2011).
8. A. Singh, S. Samanta, A. Kumar, A. K. Debnath, R. Prasad, P. Veerender, V. Balouria, D. K. Aswal, and S. K. Gupta, *Org. Electron.*, **13**, 2600-2604 (2012).
9. M. J. Jafari, M. E. Azim-Araghi, and S. Barhemat, *J. Mater. Sci.*, **47**, 1992-1999 (2012).
10. A. S. Sukhikh, T. V. Basova, and S. A. Gromilov, *J. Struct. Chem.*, **57**, No. 3, 618-621 (2016).
11. K. Vasseur, K. Broch, A. L. Ayzner, B. P. Rand, D. Cheyns, C. Frank, F. Schreiber, M. F. Toney, L. Froyen, and P. Heremans, *ACS Appl. Mater. Interfaces*, **5**, No. 17, 8505-8515 (2013).
12. T. Lei, J.-H. Dou, Z.-J. Ma, C.-H. Yao, C.-J. Liu, J.-Y. Wang, and J. Pei, *J. Am. Chem. Soc.*, **134**, No. 49, 20025-20028 (2012).
13. A. Katosouras, N. Asparini, C. Koulogiannis, M. Spanos, T. Ameri, C. J. Brabec, C. L. Chochos, and A. Avgeropoulos, *Macromol. Rapid Commun.*, **36**, No. 20, 1778-1797 (2015).
14. H. Yang, P. Bhimaraj, L. Yang, R. W. Siegel, and L. S. Schadler, *J. Polymer Sci., Part B, Polymer Phys.*, **45**, No. 7, 747-757 (2007).
15. P. Dutta, *Curr. Sci.*, **78**, No. 12, 1478 (2000).
16. E. Lifshin (ed.), *X-Ray characterization of materials*, Wiley-VCH (1999).
17. A. S. Sukhikh, T. V. Basova, and S. A. Gromilov, *Acta Phys. Pol., A*, **130**, No. 4, 889-891 (2016).
18. D. D. Klyamer, A. S. Sukhikh, P. O. Krasnov, S. A. Gromilov, N. B. Morozova, and T. V. Basova, *Appl. Surf. Sci.*, **372**, 79-86 (2016).
19. L. Ruiz-Ramirez, R. Moreno, J. Brianso, X. Solans, L. Alejandro, J. Mendieta, and J. Chinchon, *Afinidad*, **45**, 509 (1998).
20. R. G. Parkhomenko, A. S. Sukhikh, D. D. Klyamer, P. O. Krasnov, S. A. Gromilov, B. Kadem, A. K. Hassan, and T. V. Basova, *J. Phys. Chem. C*, **121**, No. 2, 1200-1209 (2017).
21. A. B. Rodriguez-Navarro, *J. Appl. Crystallogr.*, **39**, No. 6, 905-909 (2006).